In Proceedings of the Eighth International Symposium on Robotics with Applications, part of the World Automation Congress (WAC 2000), Maui, HI, June 11-16, 2000.

# MAXIMIZING THE SENSATION OF COMPLIANCE IN TELEOPERATIVE SURGERY

FRANK TENDICK
*Department of Surgery, University of California San Francisco*
*Department of Bioengineering, University of California Berkeley*

M. CENK ÇAVUŞOĞLU
*Department of Electrical Engineering and Computer Sciences*
*University of California, Berkeley*

NEEL DHRUV, ALANA SHERMAN
*Graduate Group in Bioengineering*
*University of California, Berkeley and San Francisco campuses*

## ABSTRACT

Minimally invasive surgery (MIS) can be of great benefit to the patient, but places great demands on the surgeon's perceptual motor skills. Teleoperation technology can restore some of the lost dexterity and sensation in MIS. In this paper, we describe (a) experiments to determine human capability to discriminate changes in compliance displayed through a haptic interface and (b) analysis of teleoperator control algorithms to optimize the transmission of compliance. The paradigm used in both cases is the ability to detect a change in compliance of a surface, as would occur due to a lesion or vessel embedded in soft tissue. It is shown that sensitivity to sinusoidal variations in compliance across a surface at high spatial frequencies is much better than discrimination between two compliant surfaces. A new metric for teleoperator performance is introduced which optimizes the transmission of changes in compliance while maintaining adequate stability and tracking accuracy.

**KEYWORDS:** Haptics, teleoperation, minimally invasive surgery, psychophysics.

## INTRODUCTION

Traditional surgery requires an incision large enough for the surgeon to see directly and place his or her fingers and instruments directly into the target operating site. Most often, the damage done to skin, muscle, connective tissue, and bone to reach the region of interest causes much greater injury than the curative procedure itself. This results in more pain to the patient, longer recovery times, and complications due to surgical trauma. The accelerating trend is toward minimally invasive surgery (MIS), in which unnecessary trauma is limited by reducing the size of incisions to 1 cm or

less or by using catheters or endoscopes threaded through vessels, the gastrointestinal tract, or other tubular structures. The other side of MIS, unfortunately, is that from the surgeon's point of view it is minimal access surgery. Reduced access reduces dexterity, limits perception, increases strain and the likelihood of error, and lengthens procedure time [1].

Teleoperation technology can restore some of the lost dexterity and sensation [2, 3]. Millimeter scale manipulators that fit through a cannula provide additional degrees of freedom in orientation, while external limbs control position. The surgeon uses master controllers to command the slave manipulator position, while interaction forces between the slave and tissue are reflected to the master. The teleoperator serves as a two-port interface between the surgeon and the environment inside the patient. It is then possible to design the master to provide a good interface to the properties of the surgeon's hand, such as range of motion and perceptual capabilities, while optimizing the slave manipulator to the properties of tissues, to allow maximal control and sensation with minimal trauma. Control algorithms can be designed to shape the mechanical impedance characteristics of the teleoperator.

In this paper, we describe experiments to determine human capability to discriminate changes in compliance displayed through a haptic interface and analysis of teleoperator control algorithms to optimize the transmission of compliance.

**Human Compliance Discrimination Ability.** Psychophysical experiments in haptics have focused on determining thresholds for sensation. Jones and Hunter determined Weber fractions for force, displacement, and compliance discrimination to be 0.07, 0.09 and 0.23, respectively [4]. Measured sensitivity to stiffness was less than predicted by models simply summing sensitivities to force and displacement, indicating that more complex filtering occurs prior to decision making. Tan et al. studied the dependence of compliance discrimination on work or maximum force applied [5]. When work or terminal force cues were available, subjects exhibited high sensitivities to compliance (Weber fraction 0.08); however, when work and force cues were removed, the Weber fraction for compliance discrimination was 0.22. Srinivasan and Lamotte compared compliance discrimination for compliant objects with different surfaces [6]. Subjects could readily discriminate compliance differences if the object they sampled exhibited a deformable surface. Performance dramatically decreased if compliant objects with non-deformable surfaces were presented.

**Fidelity and Stability in Teleoperation.** While many researchers have studied stability and fidelity in teleoperation, these studies have focused on contact with stiff environments. In surgery, contact with a compliant surface, such as soft tissue, is common. Designing a teleoperator controller requires a trade-off between stability and fidelity. Two-port circuit models can be used to determine stability based on the loop gain of the system [7]. An equally important criteria is the "feel" of the system. One approach to performance evaluation was investigated by Lawrence, who evaluated a system's transparency [8], defined as the ratio of the impedance transmitted to the master and the impedance of the environment. Lawrence's design goal was to keep this ratio equal to one over a maximal bandwidth. Other recent work focusing on the human interface was carried out by Daniel and McAree [9]. Their design included

a filter which fed back forces from the environment at frequencies important to the stimulation of tactile and kinesthetic receptors. While this type of filtering does provide greater stability, the design needs for a compliant surface may be different than those used for a hard contact system.

In previous experimental work, teleoperator controllers have been evaluated based on a number of performance criteria [10, 11]. The conclusions of these experiments have been that force feedback increases performance, but causes stability problems, especially under time delay. However, this previous work focused on hard contact situations, which may have stricter stability criteria than situations involving compliant surface interaction. Furthermore, time delay is not significant in teleoperative surgery for dexterity enhancement, in which the surgeon is not remote to the patient.

**Parallel Research Thrusts.** Our approach to improving the sensation of compliance as perceived through a teleoperator is twofold. First, we describe experiments performed to determine human capability to discriminate changes in compliance displayed through a haptic interface. Second, we introduce metrics and evaluate teleoperator control algorithms to optimize the transmission of compliance. The paradigm used in both cases is the ability to detect a change in compliance of a surface, as would occur due to a lesion or vessel embedded in soft tissue.

## SIMULATED SURFACE COMPLIANCE DISCRIMINATION

### Methods

Experiments were performed using computer-simulated compliant surfaces perceived through a haptic interface. The environment was implemented on a dual processor Silicon Graphics Octane workstation, while a Phantom (Sensable Technologies, Cambridge, MA) commercial 3 DOF haptic interface with force feedback provided the haptic interface. The Phantom tracks position with a resolution of 0.03 mm, uses an update rate of 1000 Hz, and produces forces with a resolution of 0.01 N after overcoming device friction determined by the manufacturer to be 0.04 N.

Subjects were presented with two simulated surfaces. One surface exhibited a sinusoidally varying compliance profile over its length while the other surface had a constant compliance. Forces were only applied to subjects' fingers in the normal (vertical) direction. Subjects were allowed to explore the virtual environment actively by scanning from side to side, enabling each subject to choose his or her strategies for discriminating between stimuli. Subjects were tested at three mean levels of compliance, 2, 4, and 8 mm/N, which roughly corresponded to measured values of compliance for pig tissues (liver, skin, and stomach, respectively) (unpublished data). Compliance contrast profiles were presented at five spatial frequencies: 0.125, 0.25, 0.5, 1.0, and 2.0 cycles/cm, which were chosen because they are within the size range of typical features that may have to be detected by palpation. We call this the *contrast detection* experiment.

In addition, each subject performed one session that measured the compliance discrimination threshold. This test consisted of subjects having to choose the softer of two surfaces. Standard levels of 2, 4, 8 mm/N were used, with the comparison surface

always more compliant than the standard. We call this the *compliance discrimination* experiment.

Psychophysical experiments were performed using a 2-down, 1-up adaptive procedure to determine compliance contrast detection thresholds with threshold corresponding to correctly detecting contrast 71% of the time [12]. The mean compliance of the surfaces was equal in the contrast detection experiment. Subjects were instructed to indicate which surface contained the sinusoidal component of compliance. The magnitude of contrast was decreased after two consecutive correct answers and increased after one incorrect response. Feedback was provided after each trial indicating if the subject got it right or wrong. After eight changes in direction, the series was terminated and a new one begun at a different spatial frequency. The estimate of threshold was then determined by averaging the magnitude of contrast at each of the eight changes in direction. The same adaptive 2-down, 1-up procedure was used in the compliance discrimination experiments.

Eight subjects were used in this study. To their knowledge, none of the subjects possessed any somatosensory abnormality. Subjects were allowed to train on one session before the collection of tests was started. Each subject performed the entire set of tests with their dominant hand. The full collection of tests was broken down into six sessions, each one consisting of two to three spatial frequencies at one mean level of compliance. Each session contained one mean level of compliance and either the two high spatial frequencies in ascending order or the three lower spatial frequencies in ascending order. The order of mean levels of compliance and low or high spatial frequencies was pseudo-randomized between subjects. In a final session, the compliance discrimination threshold was determined in the dual surface comparison test.

Experiments were carried out with subjects seated in a chair, a comfortable distance away from the viewing screen and the Phantom. A cloth drape was placed over the Phantom during trials to prevent subjects from obtaining visual cues. Subjects listened to white noise through headphones during trials to mask any auditory cues from the actuation of the motors. To guard against excessive fatigue during a session, each subject's wrist was supported by a sliding track.

## Results

The compliance contrast detection thresholds at each of the five spatial frequencies and the three mean levels of compliance were determined for each subject. This was done by averaging the contrast magnitude at the changes in direction during each series. The data from the compliance discrimination tests were similarly analyzed. Individual subjects' thresholds were subsequently averaged among all to provide the estimate of threshold. Figure 1 shows the detection thresholds for different mean levels of compliance over the range of spatial frequencies as well as the compliance discrimination results at the three standard compliances. As can be seen from the figure, compliance discrimination just-noticeable differences (JND) were determined to be 30, 17, and 13% for initial compliances of 2, 4, 8 mm/N, respectively. At higher spatial frequencies, sensitivity to compliance contrast improved dramatically, with an asymptote of about 3% contrast for all mean compliance levels. The minimal sensitivity limit appears to begin around a spatial frequency of 1 cycle/cm.

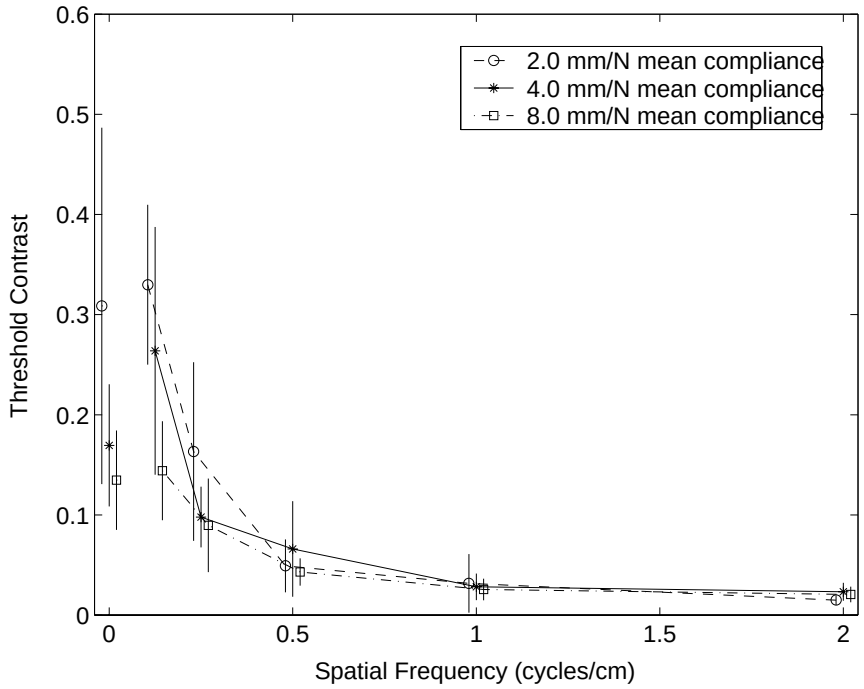


Figure 1: Compliance contrast detection and compliance discrimination thresholds averaged among all subjects, mean +/- standard deviation. Compliance discrimination results are plotted at DC, or 0 cycles/cm. Data are offset along abscissa to prevent overlapping of standard deviation bars.

### Discussion

The results that we obtained for compliance discrimination are compatible with published estimates of a JND range of 18–23% and roughly follow Weber's law for contrast detection. Of particular interest in the contrast detection experiments is the relationship between stimulus spatial frequency and the resulting temporal frequency as the subject scans across the surface. Preliminary analysis suggests that subjects used velocities in the range of 20–40 cm/s. This is comparable to the results of Peine et al. in tactile scanning experiments [13]. At these scanning rates, the higher spatial frequencies in our experiment would tend to produce stimuli in a sensitive temporal frequency range for cutaneous and kinesthetic receptors. In the second half of this paper, we introduce a metric for the frequency response of teleoperators and compare three fundamental architectures.

## COMPARISON OF TELEOPERATOR CONTROL ARCHITECTURES

### Three Architectures

The three controller architectures considered in this study are position error (PERR), kinesthetic force feedback (KFF), and position plus force feedback (P+FF) (Figure 2). In the PERR architecture, the forces sent to the master are proportional to the po-

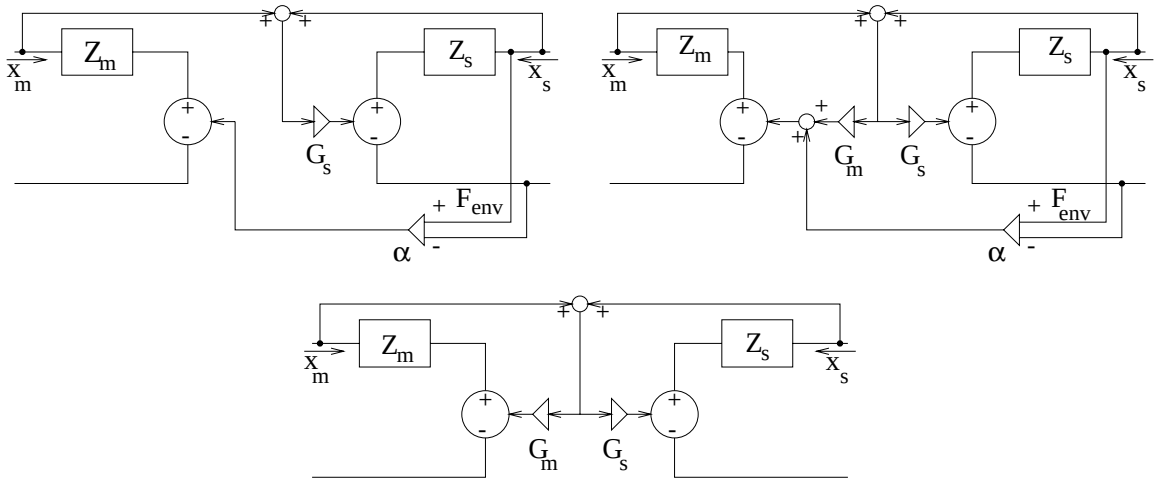


Figure 2: KFF (left), P+FF (right), and PERR (center) teleoperation architectures. The human operator would interface through the master at the left, and the slave to the right would interact with the environment in each case.

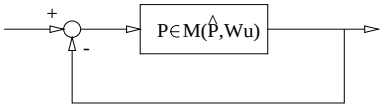


Figure 3: Closed loop system with multiplicative uncertainty.

sition error between the master and slave manipulators. The KFF architecture uses a force sensor on the slave end to transmit forces back to the master. The P+FF architecture is a hybrid of KFF and PERR in which the force fed back to the master is a linear combination of the position error and the interaction force between the slave and the environment. In all three controllers the master position is used to command the slave.

The stability-fidelity trade-off determines the controller gains for the teleoperator. In general terms, stability favors low controller gains, whereas performance favors higher gains. The following discussion outlines the analysis performed to determine the controller parameters.

The analysis uses a second-order linear model fit we have found for the Phantom interface used in the experiments described in the first half of this paper, $Z = 1/[9.64e^{-5}s^2 + (0.00266 + D_x)s + 0.0322]$, where $D_x$ is the active damping used. The same model is used for both master and slave manipulators.

## Stability

For stability analysis, we use a robust stability criterion for unstructured uncertainties as given in Zhou, Doyle, and Glover [14]. For SISO systems, the criterion is as follows.

**Theorem 1 (Robust Stability Criterion)** *Consider the closed loop system shown in Figure 3 with multiplicative unstructured uncertainty. The uncertainty is defined*

*as*

$$P \in M(\hat{P}, W_u) = \{\hat{P}(1 + W_u\Delta) : \Delta \in \mathcal{R}, \sup|\Delta(jw)| < 1, \\ \#\ of\ rhp\ poles(\hat{P}) = \#\ of\ rhp\ poles\ (\hat{P}(1 + W_u\Delta))\}, \quad (1)$$

*where $P$ is the loop gain, $\hat{P}$ is the nominal plant loop gain, $W_u$ is the uncertainty weighting function, and $\mathcal{R}$ is the set of proper real rational functions. Then, the closed loop system shown is stable for all $P \in M(\hat{P}, W_u)$, if and only if it is stable for the nominal plant $\hat{P}$, and $\|W_u T\|_\infty \leq 1$, where $T = \frac{\hat{P}}{1+\hat{P}}$.*

The uncertainty weighting function $|W_u(jw)|$ can be interpreted as the percentage uncertainty in $\hat{P}$ at the frequency $w$.

The teleoperator can be modeled as a two-port network element relating force and velocity of the human operator, $F_{ho}$ and $V_{ho}$, to the environment, $F_e$ and $V_e$. We follow Hannaford [7] in using the hybrid parameters to characterize system behavior:

$$\begin{bmatrix} F_{ho}(s) \\ V_e(s) \end{bmatrix} = \begin{bmatrix} H_{11}(s) & H_{12}(s) \\ H_{21}(s) & H_{22}(s) \end{bmatrix} \begin{bmatrix} V_{ho}(s) \\ F_e(s) \end{bmatrix} \quad (2)$$

For the teleoperator, the loop gain P is calculated in Hannaford as

$$P = \frac{H_{12}H_{21}Z_e}{(H_{11} + Z_{ho})(1 + H_{22}Z_e)} \quad (3)$$

where $Z_e$ and $Z_{ho}$ are respectively the environment and human operator impedances.

For this analysis we only consider the uncertainty in the environment. Since $Z_e$ shows as $\frac{Ze}{1+H_{22}Z_e}$ in the loop gain expression, we put an upper bound on the variation in this term for the possible set of environments:

$$Z_e \in \{(B_e s + 1)K_e : B_e \geq 0.05, 0 \leq K_e < \infty\}. \quad (4)$$

Since we want to have the nominal environment $\hat{Z}e$ for $\Delta = 0$, we pick

$$W_u\Delta = \frac{1 + H_{22}\hat{Z}_e}{\hat{Z}e}\frac{Z_e}{1 + H_{22}Z_e} - 1 = \frac{1}{H_{22}\hat{Z}_e}\frac{Z_e - \hat{Z}e}{1 + H_{22}Ze} \quad (5)$$

then we pick a frequency dependent upper bound to $|\frac{Z_e - \hat{Z}_e}{1+H_{22}Z_e}| < |\Phi(jw)|$ for the possible environment and controller values, which gives $W_u = \frac{1}{H_{22}\hat{Z}_e}\Phi$.

The stability of the PERR and KFF architectures as a function of their parameters is shown in Figure 4. As expected, these figures show that the system becomes more stable when the gains are decreased. Due to the effects of the unmodeled uncertainties, e.g. human operator impedance and sensor noise, we use a stricter stability constraint than given in Theorem 1: $\|W_u T\|_\infty \leq \frac{1}{3} < 1$.

## Performance

Once the stability criterion has been met, the performance of the controller is evaluated. Position tracking and fidelity are the two measures employed to determine the performance of the controllers. Tracking is a measure of how well the slave

manipulator can follow the position commanded by the master manipulator. Traditionally transparency, which is defined as the ratio of the transmitted impedance to the environmental impedance, is used as a fidelity measure[8]. In this paper, we propose a different fidelity measure which focuses on the sensitivity of the transmitted impedance to changes in the environmental impedance rather than transparency. This measure will correspond to the ability of a surgeon to discriminate changes of compliance in the environment. We find the gains for each controller architecture that form the subset that *meet* stability and tracking requirements, and then choose particular gains that *optimize* fidelity.

**Tracking Analysis.** One important requirement for the teleoperator is to have a good tracking performance in free space. One can quantify this tracking performance in terms of an upper bound on the disturbance sensitivity function of the forward position loop. For all of the teleoperation architectures used, the disturbance sensitivity function $(1 - H_{21})$ is given by $S = Z_s/(Z_s + G_s)$, where $Z_s$ is the slave manipulator's impedance and $G_s$ is the slave controller.

To measure the tracking performance of the system a frequency dependent upper bound for the allowable disturbance sensitivity is established: $|S(jw)| < |b(jw)|$. This upper bound is placed such that each control architecture exhibits good disturbance rejection in the low frequency range, frequencies less than 5 Hz. This value should safely encompass the range of frequencies for operator movement. The tracking condition is satisfied if and only if $\|W_p S\|_\infty \leq 1$, where $W_p = 1/b$.

For each controller architecture the same upper bound, $b(jw)$, is placed on the sensitivity function. The general trend of this constraint is to favor controllers with higher gains on the slave. Those sets of gains which meet the nominal performance requirement are then evaluated for fidelity.

**Fidelity.** The measure of fidelity proposed in this analysis is the sensitivity of the transmitted impedance to changes in the environmental impedance, defined as:

$$\left\| W_s \left. \frac{dZ_t}{dZ_e} \right|_{Z_e = \hat{Z}_e} \right\|_2 \tag{6}$$

where $W_s$ is a frequency dependent weighting function, chosen as a low pass filter in this study. The cutoff frequency used is 40 Hz, based on the effective stimulus temporal frequencies at typical scanning rates in the compliance discrimination experiments. Figure 4 illustrates how the fidelity increases as the controller gains increase for the KFF and PERR architectures.

The results show that the fidelity is best for P+FF, then KFF and finally PERR (Figure 5). It is interesting to note that the cutoff frequency of the weighting function is critical in determining which controller has the best fidelity. For a lower frequency range, PERR has slightly better fidelity than KFF.

## DISCUSSION

The dependence of compliance sensitivity on spatial frequency is probably due to the resulting temporal frequency of the stimulus as the subject scans across the sur-

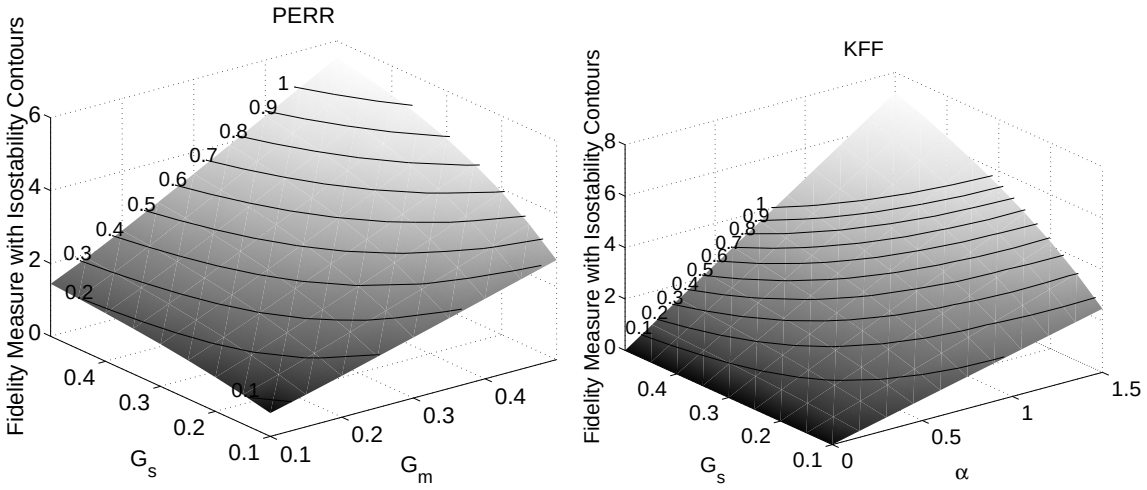


Figure 4: Fidelity of the PERR and KFF architectures as a function of controller parameters. Contours of constant stability are shown overlaid on the fidelity surface for comparison. Note that stability decreases as fidelity increases.

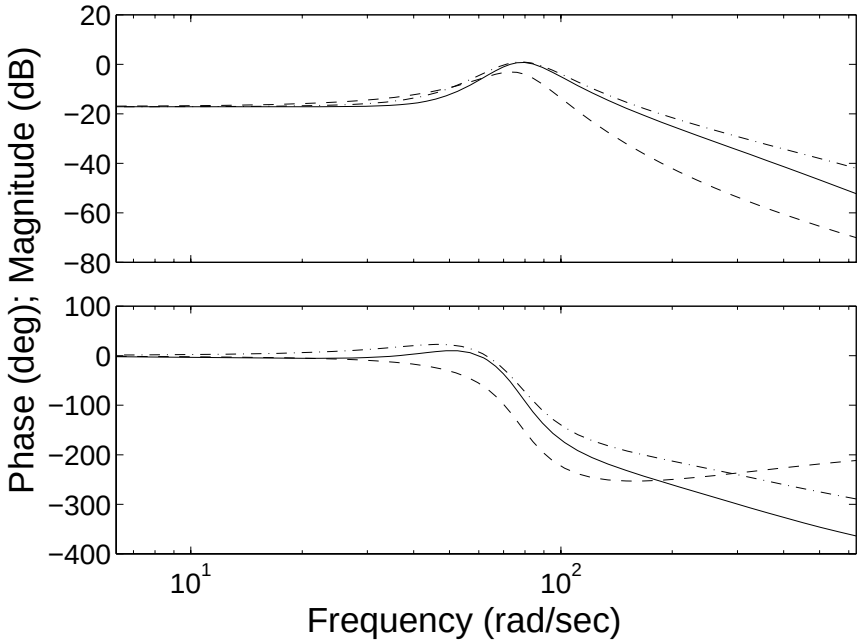


Figure 5: Frequency dependence of (unweighted) transmitted impedance sensitivity $dZ_t/dZ_e$ at $Z_e = \hat{Z}_e$. Solid line: KFF, dashed line: PERR, dash-dot line: P+FF.

face. We are now performing experiments to elucidate the frequency dependence based on receptor and display characteristics. This will provide data to adjust the weighting for the teleoperator fidelity metric. We have found the stability and performance measures to depend sensitively on system parameters such as sensor noise that are difficult to identify. Consequently, experimental verification of the algorithms is essential. For this we will measure subjects' ability to detect inclusions such as rubber tubes embedded in a soft gel. Finally, the performance metric will allow us to optimize the design of future telesurgical systems that extend capabilities using novel actuators and sensors.

**ACKNOWLEDGMENT:** This work was supported in part by the National Science Foundation under grants IRI-95-31837 and CDA-97-26362.

# References

[1] F. Tendick, R. Jennings, G. Tharp, and L. Stark, "Sensing and manipulation problems in endoscopic surgery: experiment, analysis and observation," *Presence*, vol. 2, pp. 66–81, Winter 1993.

[2] M. Cavusoglu, F. Tendick, M. Cohn, and S. Sastry, "A laparoscopic telesurgical workstation," *IEEE Trans. Robotics and Automation*, vol. 15, no. 4, pp. 728–39, 1999.

[3] J. W. Hill, P. S. Green, J. F. Jensen, Y. Gorfu, and A. S. Shah, "Telepresence surgery demonstration system.," in *Proc. IEEE Intl. Conf. Robotics and Automation*, pp. 2302–7, 1994.

[4] L. Jones and I. Hunter, "A perceptual analysis of stiffness," *Exp. Brain Res.*, vol. 79, pp. 150–6, 1990.

[5] H. Tan, N. Durlach, G. Beauregard, and M. Srinivasan, "Manual discrimination of compliance using active pinch grasp: the roles of force and work cues," *Perception and Psychophysics*, vol. 57, no. 4, pp. 495–510, 1995.

[6] M. Srinivasan and R. LaMotte, "Tactual discrimination of softness," *J. Neurophys.*, vol. 73, pp. 88–101, 1995.

[7] B. Hannaford, "Stability and performance tradeoffs in bi-lateral telemanipulation," in *Proc. IEEE Intl. Conf. Robotics and Automation*, (Scottsdale, AZ), pp. 1764–1767, 1989.

[8] D. Lawrence, "Stability and transparency in bilateral teleoperation," *IEEE Trans. Robot. Autom.*, vol. 9, no. 5, pp. 624–37, 1993.

[9] R. Daniel and P. McAree, "Fundamental limits of performance for force reflecting teleoperation," *Intl. J. Robotics Research*, vol. 17, no. 8, pp. 811–30, 1998.

[10] H. Das, H. Zak, W. Kim, A. Bejczy, and P. Schenker, "Operator performance with alternative manual control modes in teleoperation," *Presence*, vol. 1, pp. 201–218, winter 1992.

[11] B. Hannaford and R. Anderson, "Experimental and simulation studies of hard contact in force reflecting teleoperation," in *IEEE International Conference on Robotics and Automation*, pp. 584–9, 1988.

[12] N. Macmillan and C. Creelman, *Detection theory : a user's guide*. New York, NY: Cambridge University Press, 1991.

[13] W. Peine, P. Wellman, and R. Howe, "Temporal bandwidth requirements for tactile shape displays," in *Proc. ASME Dynamic Systems and Control Division* (G. Rizzoni, ed.), (Dallas, TX), pp. 107–14, 1997.

[14] K. Zhou, J. C. Doyle, and K. Glover, *Robust and Optimal Control*. New Jersey, USA: Prentice-Hall, Inc., 1996.